3D printed elastic honeycombs with graded density for tailorable energy absorption

Simon R. G. Bates[1], Ian R. Farrow[2], Richard S. Trask[3]

[1, 2] Advanced Composites Centre for Innovation and Science (ACCIS), Department of Aerospace Engineering, University of Bristol, Queens Building, University Walk, Bristol, BS8 1TR, UK.

[3] Department of Mechanical Engineering, University of Bath, Claverton Down, Bath, BA2 7AY, UK.

[1] Simon.R.G.Bates@bristol.ac.uk

[2] Ian.Farrow@bristol.ac.uk

[3] R.S.Trask@bath.ac.uk

Keywords: Cellular structures, Elastomers, functional grading, energy absorption

ABSTRACT

This work describes the development and experimental analysis of hyperelastic honeycombs with graded densities, for the purpose of energy absorption. Hexagonal arrays are manufactured from thermoplastic polyurethane (TPU) via fused filament fabrication (FFF) 3D printing and the density graded by varying cell wall thickness though the structures. Manufactured samples are subject to static compression tests and their energy absorbing potential analysed via the formation of energy absorption diagrams. It is shown that by grading the density through the structure, the energy absorption profile of these structures can be manipulated such that a wide range of compression energies can be efficiently absorbed.

1 INTRODUCTION

Cellular structures such as polymeric foams and expanded honeycombs are used across all industries where persons or components must be protected from vibrational or impact loads. Polymeric foams are particularly attractive as passive protection systems as they are relatively cheap, easily formed into complex geometries and can effectively dissipate the energy of repeated impact events [1]. Large amounts of energy is dissipated in such structures via cell wall buckling, through viscous losses in the movement or compression of fluid in the structure, via plastic deformation and by fracture [2]. The typical compressive stress-strain behaviour of an elastic cellular structure is shown in Figure 1 with the energy absorbed per unit volume indicated in a plateau region. It is important to note that there exists a given energy for any cellular structure to which it is optimally suited to absorb; this is the energy that compresses the structure to the point just before densification, at the end of the stress plateau. Larger compression energies will densify the structure, transferring high stresses and lower compression energies could be more efficiently absorbed by a lower density structure.

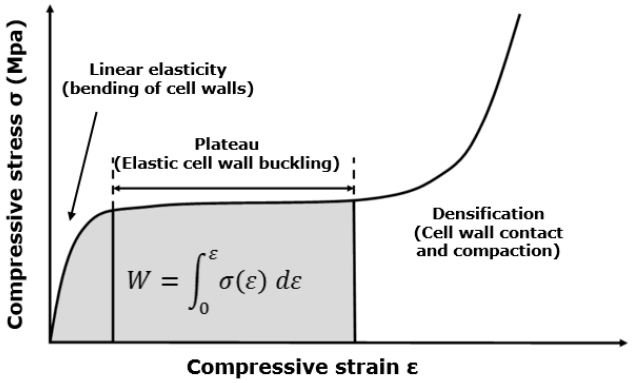

Figure 1: Schematic illustrating the typical compressive stress-strain behaviour of an elastic cellular structure

The energy absorbing capability of a cellular structure in compression can be illustrated by plotting the cumulative area under the stress strain curve against stress [2]. Figure 2a shows an example of characteristic energy absorption curves for cellular structures with a range of densities.

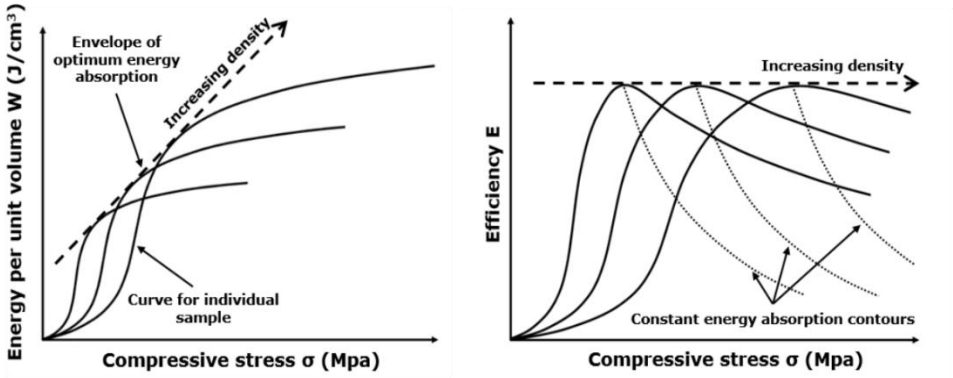

Figure 2: a) Schematic illustrating the energy absorption-stress profile of three cellular structures in compression made from the same material but with increasing density and b) the efficiency-stress of the same

The Optimum energy absorption envelope can be drawn that passes through the shoulder points for cellar structures formed from the same material, with increasing density. The Efficiency of such structures at absorbing a range of impact energies can then be defined by dividing the energy absorbed by instantaneous stress [3] as shown in Figure 2b.

Despite their energy dissipating merits, there is only a narrow range of impact energies which a single density cellular structure will efficiently absorb. In real world applications, energy absorbing structures are likely to be subject to a large range of vibrational loads and therefore a more considered approach to cellular structure design is required that addresses this. In this work, we explore how functionally grading the density of cellular structures can be used to manipulate their energy absorbing response.

3D printing provides a geometric design freedom that not achievable via any other means [4] making it the ideal method of manufacture to consider for the creation of these tailored cellular structures. Although there have been a number of attempts to create 3D printed cellular structures with tailorable stress-strain and energy absorbing behaviour [5-7], much of the work has focused on the printing of brittle structures and attempts to create structures with hyperelastic behaviour via polyjet 3D printing produced samples fragile in nature which fractured during the removal of support material [8]. In order to create hyperelastic, durable structures, fused filament fabrication (FFF) 3D printing is used as it allows the use of thermoplastic polyurethane (TPU), a material known to have excellent impact properties and abrasion resistance [9].

2 MATERIALS AND METHODS

2.1 3D printing of cellular arrays

The cellular structures in this study were produced via FFF 3D printing using the Ultimaker Original desktop 3D printer. Thermoplastic polyurethane (TPU) produced by Fenner drives Inc (NinjaFlex) was used as the feedstock material. Prior testing has shown that the 3D printed TPU has a density, ρ_S=1235kg/m^3, ultimate tensile strength, σ_{UTS}=40MPa and tensile strain to failure of up to 700%. The material was also observed to be exhibit hysteresis, strain rate dependence and undergo strain softening upon cyclic loading which has been previously reported for TPUs [9].

2.2 Cellular array design:

Four specimens with graded density through their structure were produced along with three specimens of constant density for reference. All graded cellular arrays were designed with wall length, l=4.65mm and an average cell wall thickness, t_a=1.6mm. The wall thicknesses were graded through the structures from t=0.8mm to t=2.4mm; Figure 3a) and 3b) show a design schematic and a manufactured specimen respectively and 3c) i)-iv) details the wall thicknesses for the continuously, 5-stage, 3-stage and 2-stage graded structures respectively. The low, medium and high density reference samples were designed with wall length, l=4.65mm and thicknesses of t=0.8, 1.6 and 2.4mm respectively.

The relative density for a hexagonal array with constant wall length and thickness is equal to $\rho_{RD}=(2/3^{-2})(t/l)$ [2] and for a graded structure designed, it holds that the average relative density, $\rho_{aRD}=(2/3^{-2})(t_a/l)$. The measured relative density, ρ^*_{aRD} of the final 3D printed specimens were calculated such that $\rho_a/\rho_S=\rho^*_{aRD}$ where ρ_a=specimen mass/the cuboidal area which it occupies. The wall thickness of the produced parts were measured to be accurate to within ±0.2mm of the design values. Table 1 gives details of the dimensions, relative density and number of rows of hexagonal cells in the manufactured specimens.

Table 1: Properties of the cellular arrays manufacture via FFF 3D printing.

Specimen details	Number of rows	Height, h (mm)	Width, w (mm)	Depth, d (mm)	Relative density, ρ^*_{aR} (-)
High density	19	66.2	81.7	29.8	0.50
Medium density	19	65.5	81.1	29.7	0.37
Low density	19	64.5	80.7	29.6	0.26
Continuous grading	19	65.4	81.1	29.7	0.39
5-stage grading	21	72.5	81.2	29.7	0.37
3-stage grading	19	65.5	81.1	29.6	0.38
2-stage grading	21	72	81.7	29.8	0.37

2.3 Experimental methods

Flat-plate compression tests of the hexagonal arrays were carried out using a Shimazu AGS-X static test machine with a load cell with ±10kN load cell. All samples were compressed in the -*z* direction as indicated in Figure 3a) under displacement control at strain rates, $\dot{\varepsilon}$ =0.03 up to a maximum load of 5kN to ensure complete densification. All samples were loaded and unloaded under these conditions for 5 cycles with data shown here being captured on the 5th compressive cycle. No material failure was observed during testing.

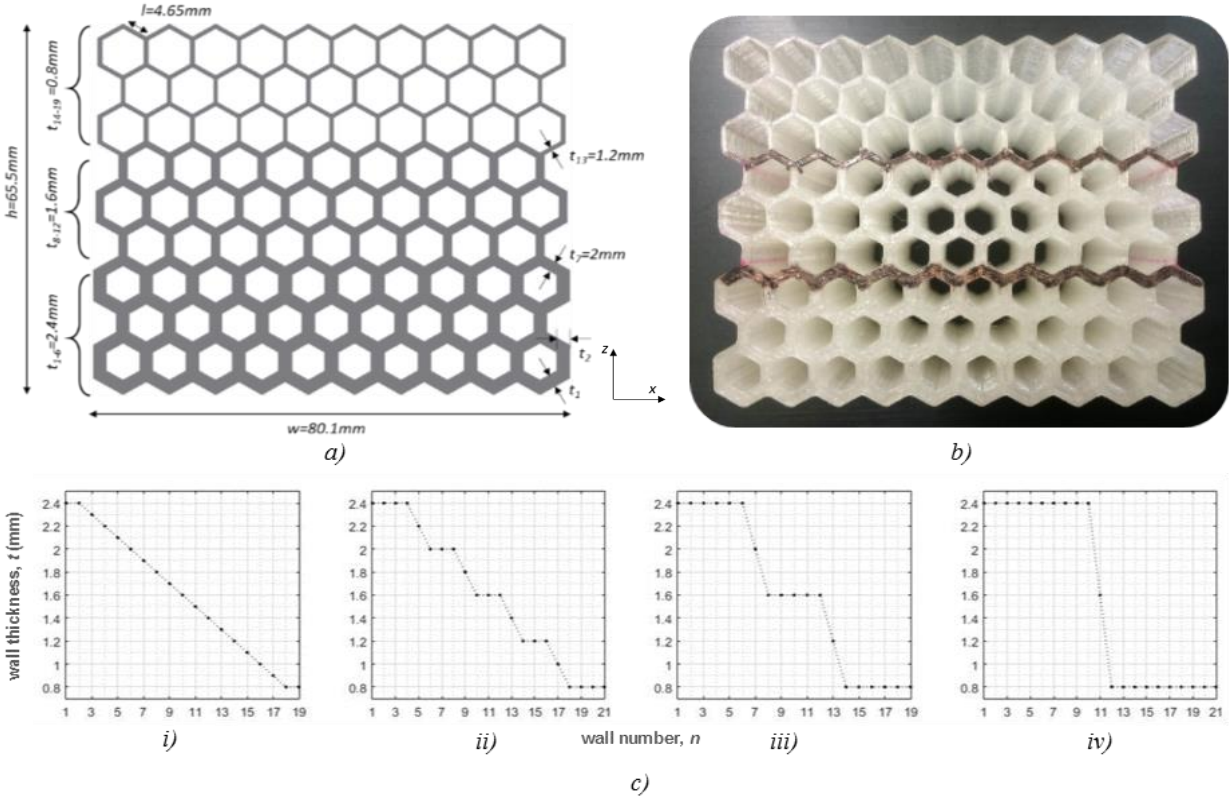

Figure 3: a) Design details of the 3-stage graded hexagonal structure. Cell walls are numbered *n*=1-19 from the base of the structure and corresponding thickness values, t_n are indicated; b) the test specimen produced by FFF 3D printing from TPU; the walls of intermediate thickness are indicated in black; c) graphical representation of the wall thickness of *c)i)* Continuous, *c)ii)* 5-stage, *c)iii)* 3-stage and *c)iv)* 2-stage graded specimens.

3 RESULTS AND DISCUSSION

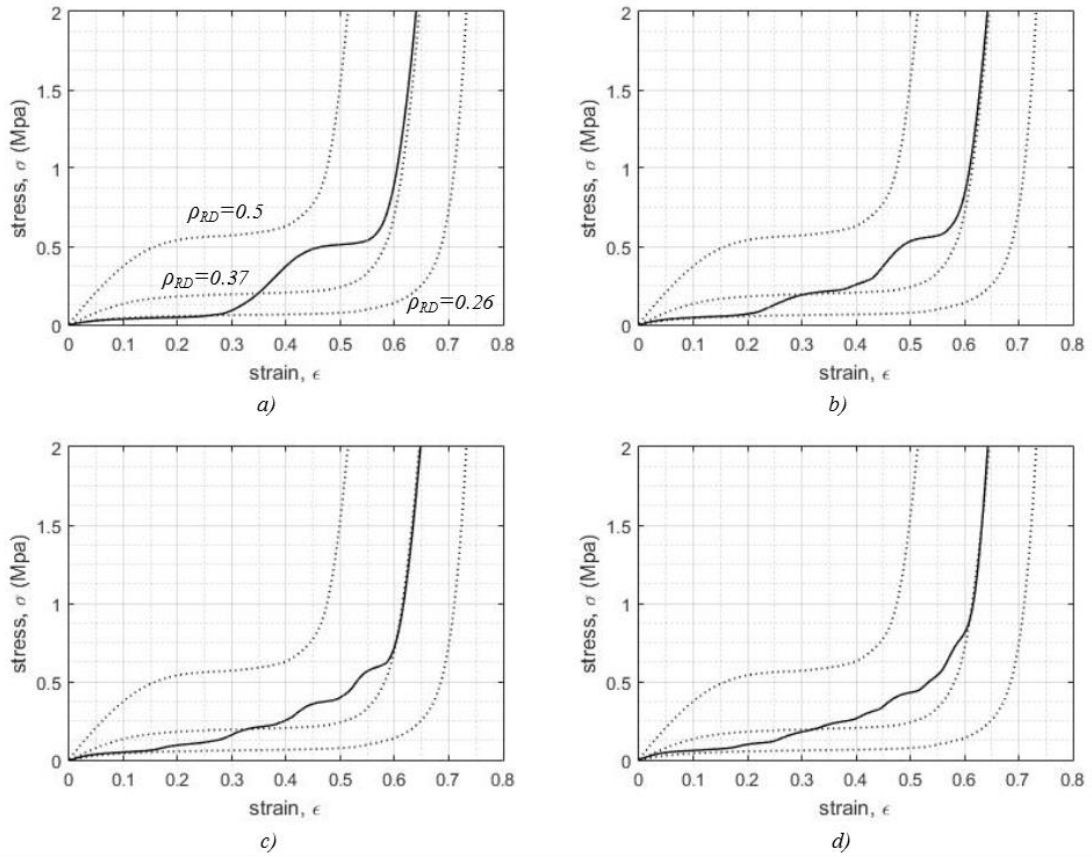

Figure 4: Stress strain behaviour of the a) 2-stage; b) 3-stage; c) 5-stage and d) continuously graded structures. The stress strain behaviour for the low, medium and high density structures are included for reference with the relative density, ρ_{RD} indicated in a).

3.1 Stress-strain and cellular collapse behaviour

3.1.1 Uniform structures

In Figure 4, stress-strain ($\dot{\varepsilon}$ =0.03s^{-1}) curves are plotted for the four graded structures with the stress-strain curves for the three uniform density structures included for reference. The uniform density structures exhibit flat plateau sections which occur at higher stresses and over shorter lengths with increasing density. The definition of the length of the plateau sections can be ambiguous however in this case we shall define the end of the plateau to the strain at which the corresponds to the maximum energy absorbing efficiency; the definition of this point is discussed further in section 3.2 and marks the point at which the onset of densification occurs. The onset of the plateau shall be approximated here as 0.1 strain which corresponds to the theoretical collapse stress for regular hexagons [2] and the plateau stress, σ_p defined as stress at the median plateau strain. With these definitions the low, medium and high density structures have plateaus which span 0.43, 0.38 and 0.31 strain and have plateau stresses of σ_p= 0.05, 0.19 and 0.56MPa respectively. Beyond strains of 0.47, 0.6 And 0.78 the low, medium and high density structures respectively approach a common stiffness profile and at this point they are regarded to have reached full densification. The corresponding stresses at which the uniform structures reach full densification are at σ_d=0.9, 0.63 and 0.4MPa respectively. The collapse behaviour of the medium density array that corresponds to this data can be seen in Figure 5a).

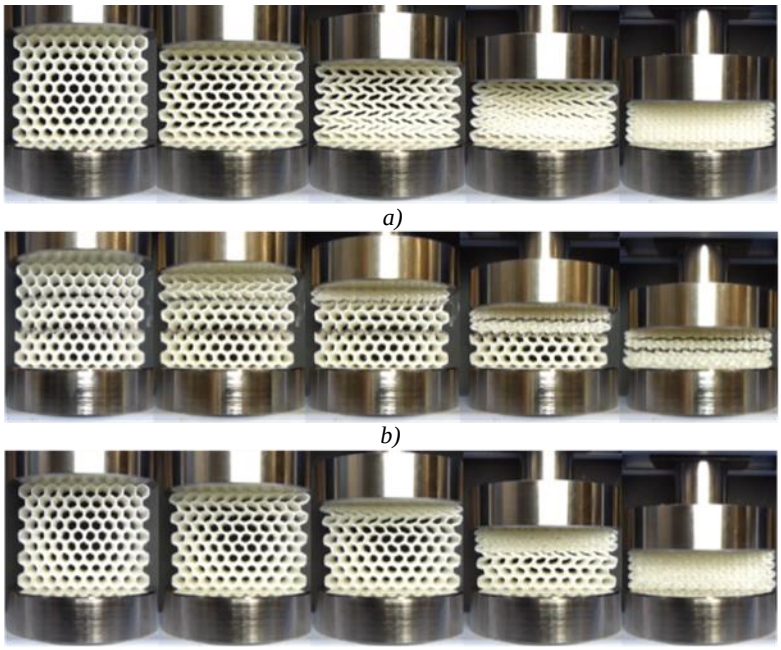

Figure 5: The cellular collapse behaviour during static compression of the a) medium density array ($\rho_{RD}=0.37$); b) 3-stage graded array and c) the continuously graded array.

3.1.2 Graded structures

The stress-strain behaviour of the 2-satge, 3-stage, 5-stage and continuously graded structures are shown in Figure 4a)-c) respectively. Clear plateau regions can be observed for the 2-stage and the 3 stage graded arrays indicating a staggered collapse of regions with increasing density within the structure during compression. The clearly defined plateaus are an indication that each density region undergoes linear deformation, collapse and densification before the succeeding, higher density layer undergoes significant deformation; Figure 5b) shows this developing collapse behaviour of the 3-stage graded array under compression, exhibiting this behaviour. The maximum stiffness in the plateau transition region is equal to the low strain stiffness of a uniform array with the density equal to the region being successively compressed. The 5-stage and continuously graded structures have less well defined plateau regions which occurs due to the onset of significant deformation of the successive, higher density layers before the previous region has undergone full densification. This behaviour can be seen in Figure 5c) which shows the compression of the continuously graded array. It can be seen that, although collapse progresses in a layer-wise manner through the structure, significant deformation of higher density rows can be observed before the full densification of the previous.

In all the graded arrays, the length of the individual plateaus decrease as the densities of the layers being compressed increases. The total strain to full densification of each graded structure can be seen to be approximately equal to that of the uniform structure with the same average density, where in each case, the same stiffness profile is tended to, when full densification occurs. Figure 5b) shows visually how the three layers (increasing in density from top to bottom) which begin with the same initial vertical height, compress into 3 densified layers of varying thickness; the total thickness ultimately being equal to the thickness of the equivalent uniform array with the same average density at full densification.

We have shown here that the stress strain profiles of cellular arrays may be manipulated by varying cell wall thickness through the sample without effecting the ultimate strain to densification. We have also shown how by decreasing the density grading step size, the compressive stress-strain response of the graded structure moves from a series of clearly defined stress plateaus into a more continuous response. It is hypothesised that if the

increase in *t* through the structure were to be in smaller increments, lowering the density gradient, this response would tend to a smoother line with a function relating to the low strain stiffness of each layer. In order to understand how the stress-strain behaviour of these graded structures relates to their energy absorbing capability, it is necessary to form energy absorption diagrams.

3.2 Energy absorption diagrams

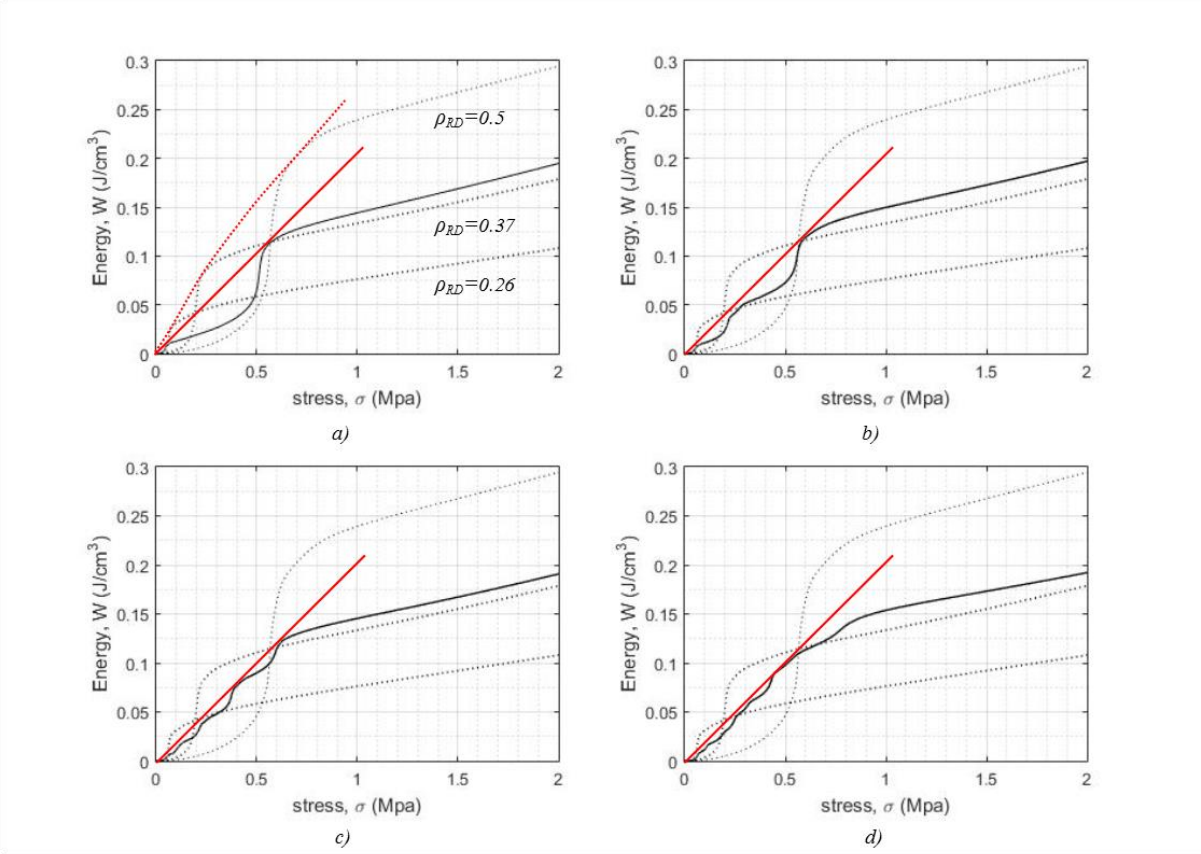

Figure 6: Energy absorption diagrams for a) 2-stage; b) 3-stage; c) 5-stage and d) continuously graded structures with the energy absorption profiles for low, medium and high density uniform structures included for reference. The optimum energy absorption envelope for the uniform structures and the approximate optimal energy absorption envelope for the individual graded structures are shown by the dotted and solid red lines respectively.

3.2.1 Uniform structures

In Figure 6, energy-stress curves are plotted for the four graded structures with the energy-stress curves for the three uniform density structures included for reference. The energy-stress curves of the three uniform density structures have a single shoulder point which corresponds to a point of optimum energy absorption efficiency [2]. The shoulder points of the three uniform density results are the points which intersect with the optimum energy absorption envelope, indicated in 6a) by the dotted red line. Each of these points indicate the compression energy that the structure is most suited to absorb, which corresponds to the stress at the point when densification begins to occur; it can be seen that compression energies above this value would lead to much larger stresses being transferred. The total useful energy, W_E absorbed by each uniform structure increases non-linearly with increased sample density with, W_E= $20x10^{-3}$, $80x10^{-3}$ and $190x10^{-3}$ J/cm^3 absorbed at stress, σ_E=0.06, 0.23 and 0.65 MPa for the low, medium and high density structures respectively.

3.2.2 Graded structures

The energy absorption capability of a graded structure should be defined by the total amount of useful energy absorbed, by the characteristics of the stress-energy profile of the array up until densification and the positioning of the energy absorption profile relative to the uniform density equivalent. In all cases, the total amount of energy absorbed by the graded structures is higher than that of the equivalent uniform structure by an average of $14.7x10^{-3}$ J/cm^3 more energy being absorbed at a compressive stress of 1MPa. The cause for this higher total energy absorption, despite the samples having the same average density, likely stems from the non-linear relationship between the structural density and energy absorption.

The energy absorption profiles of the graded structures reflect the fluctuations in the stress-strain profiles such that the energy-stress curves of the graded structures have a series of shoulder points rather than a singular shoulder; the number of shoulder points is equal to the number of graded layers through the structure. The shoulder points are well defined for the 2-stage, 3-stage and 5-stage graded structures and an optimum energy absorption envelope can be drawn for each of these individually. In the case of these graded arrays, the energy absorption envelopes can be approximated by a line which passes through the intersecting points of the uniform density energy absorption curves, as shown in Figure 6a-c). Due to the limited number of samples tested here, it is not possible to say whether the approximation may be more widely applied to arrays with graded density. For the array with continuous grading the shoulder points have converged and the energy absorption envelope is not as closely approximated by this a linear function. The ideal energy absorbing structure absorbs large amounts of energy while transferring a low stress and therefore the further to the left of the energy absorption diagram the

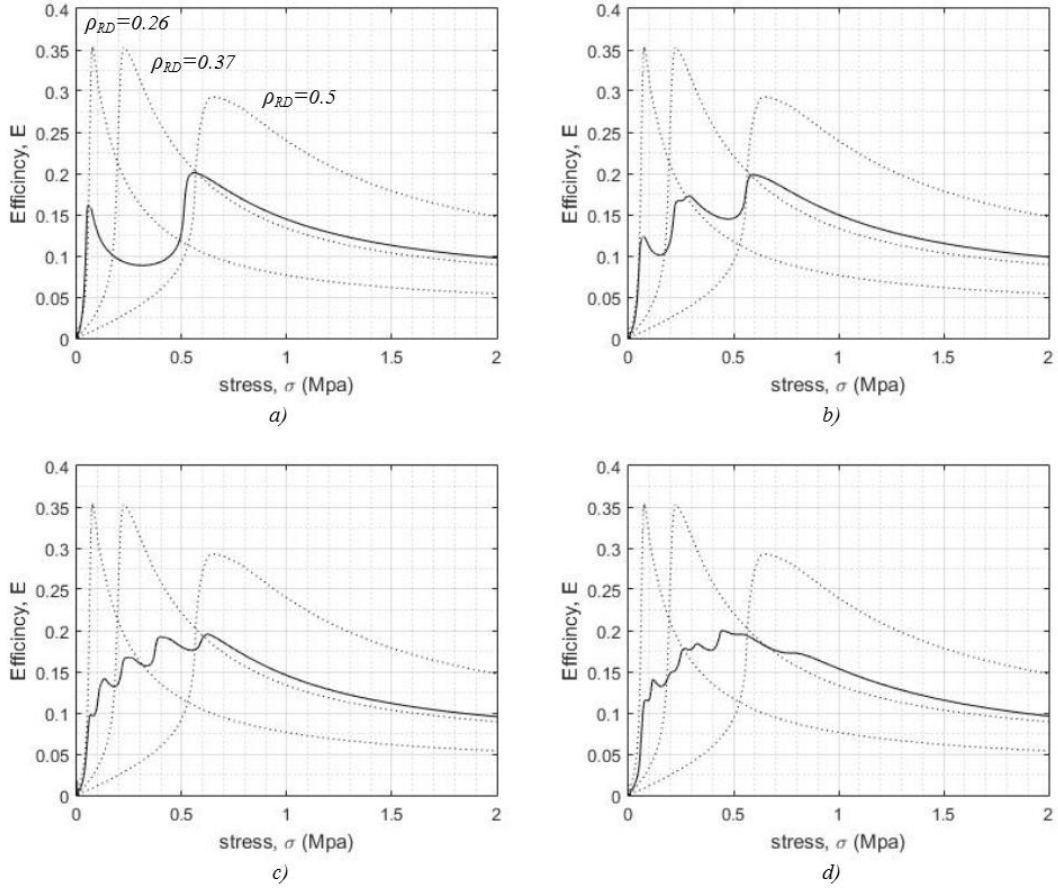

Figure 7: Efficiency-stress diagrams for a) 2-stage; b) 3-stage; c) 5-stage and d) continuously graded structures with the efficiency absorption profiles for low, medium and high density uniform structures included for reference.

points on an energy absorption curve lie, the more efficient the structure. At energies below $17x10^{-3}$, $18x10^{-3}$, $24x10^{-3}$ and $26x10^{-3}$ J/cm^3 and above $115x10^{-3}$, $115x10^{-3}$, 116 $x10^{-3}$ and $119x10^{-3}$ J/cm^3, the 2-stage, 3-stage, 5-stage and continuously graded arrays respectively lie to the left of the energy absorption curve of the medium density array. In these regions, the graded structures are more efficient at absorbing energy than the uniform structure. In the case of the arrays studies here, a larger number of densities through the structure leads to a larger portion of the energy absorption curve lying to the left of curve of the medium density array. At intermediate energies however, the uniform array is significantly more efficient at absorbing compressive energy. In order to better interpret the efficiency of these structures over a range of compression energies, efficiency diagrams can be formed by dividing the cumulative energy by the instantaneous stress [3].

3.3 Efficiency diagrams

3.3.1 Uniform structures

In Figure 7a)-d), efficiency-stress curves are plotted for the four graded structures with the efficiency-stress curves for the three uniform density structures included for reference. The efficiency parameter plotted here against stress has maxima at points just before the point where the increase in energy is exceeded by the increase in stress [1]; these maxima correspond to the shoulder points on the energy-stress graph and thusly the stress at the point of the end of the stress-strain plateau. The uniform structures all possess a single maxima, with the low and medium density structures operating at a maximum efficiency of 0.35. The efficiency of the high density structure is significantly lower at 0.29 which is due to the compressive stress-strain profile exhibiting a less well defined plateau; a result of the deformation mechanisms becoming less buckling dominated due to the high *t/l* ratio within the array.

3.3.2 Graded structures

Many of the same conclusions reached in the analysis of the graded structures via the energy absorption diagram can be reached by assessing the efficiency diagram. The efficiency curve for each graded structure has a number of peaks and it is clear that all the graded structures are more efficient at absorbing low and high energy loads whilst intermediate loads are better absorbed by the equivalent uniform structure. It can be seen that the 2-stage graded array is the most efficient out of the graded arrays at absorbing low energy loads with a peak efficiency of 0.16 at a stress of 0.055MPa however there is a large trough in efficiency at intermediate compression energies. The continuously graded structure does not exhibit the same trough in efficiency, exhibiting higher efficiency over a wider range of compression energies, with the lowest fluctuation in energy absorbing efficiency. It can also be observed that the magnitude of the efficiency peaks increases successively with the compression of the successive, higher density layer in all the graded structures.

4 Conclusions and further work

In this study we have detailed the manufacture and analysis of density graded, hyperelastic 3D printed cellular arrays for the purpose of energy absorption. In summary, the following conclusions can be drawn:

- Hexagonal cellular arrays were successfully manufactured from thermoplastic polyurethane (TPU) via the method of fused filament fabrication (FFF) 3D printing. Uniform density and graded density structures were fabricated with the resulting structures having manufactured dimension to within 0.2mm of those designed. Density grading of the structures was carried out by varying the cell wall thickness whilst maintaining the cell wall length in 2-satges, 3-stages, 5-stages or continuously through the specimen thickness.

- Stress-strain behaviour, Energy-absorption diagrams and Efficiency-stress behaviour were plotted from data gathered from static compression tests. All arrays showed no signs of visual damage after 5-compression cycles up to full densification and energies of up to $190x10^{-3}$ J/cm^3 were efficiently absorbed.

- By grading the structures, we were successful in absorbing a higher total energy in compression than the equivalent uniform array and the graded structures were also more efficient than the equivalent uniform array at absorbing low energy compression loads. The continuously graded array performed most efficiently over the widest range of compression energies however the equivalent uniform density array had the highest peak efficiency.

- Further static and cyclic testing of wider range of graded structures is required in order for more generalised conclusions to be drawn with regards to the energy absorption and dissipation behaviours of these types of structures. Other modifications the cellular arrays such as pre-buckling of cell walls and hierarchical structural grading should be looked to as methods for further tailoring the energy absorption response of these types of cellular, energy absorbing structures.

ACKNOWLEDGMENTS

This work has been financially supported by the Engineering and Physical Sciences Research Council (EPSRC) and the Royal National Lifeboat Institution (RNLI). The Authors would also like to thank the RNLI for their continued support and involvement with the progression of this work.

REFERENCES

[1] Avalle, M., Belingardi, G., & Montanini, R. (2001). Characterization of polymeric structural foams under compressive impact loading by means of energy-absorption diagram. *International Journal of Impact Engineering, 25*(5), 455-472.

[2] Gibson, L.G. & Ashby, M.F. (1999). Cellular Solids: Structure and Properties. *Cambridge University Press*.

[3] Miltz J. & Ramon O. (1990). Energy absorption characteristics of polymeric foams used as cushioning materials. *Polymer Engineering Science*, 30(2), 129-133.

[4] Hopkinson, N., Hague, R.J.M., & Dickens, P. M. (2006), Rapid Manufacturing: An Industrial Revolution for the Digital Age. *Wiley*

[5] Brennan-Craddock, J., Brackett, D., Wildman, R., & Hague, R. (2012). The design of impact absorbing structures for additive manufacture. *Journal of Physics: Conference Series*, 328

[6] Correa, D. M., Klatt, T., Cortes, S., Haberman, M., Kovar, D., & Seepersad, C. (2015). Negative stiffness honeycombs for recoverable shock isolation. *Rapid Prototyping Journal*, *21*(2), 193–200.

[7] Ajdari, A., Jahromi, B. H., Papadopoulos, J., Nayeb-hashemi, H., & Vaziri, A. (2012). Hierarchical honeycombs with tailorable properties, *International Journal of Solids and Structures*, 49, 1413–1419.

[8] Shen, J., Zhou, S., Huang, X., & Xie, Y. M. (2014). Simple cubic three-dimensional auxetic metamaterials. *Physica Status Solidi (B) Basic Research*, *251*(8), 1515–1522.

[9] Yi, J., Boyce, M. C., Lee, G. F., & Balizer, E. (2006). Large deformation rate-dependent stress–strain behavior of polyurea and polyurethanes. *Polymer*, *47*(1), 319–329.